Talanta 256 (2023) 124309

Contents lists available at ScienceDirect

Talanta

journal homepage: www.elsevier.com/locate/talanta

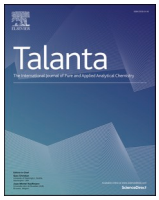

AF4-UV/VIS-MALS-ICPMS/MS for the characterization of the different nanoparticulated species present in oligonucleotide-gold nanoparticle conjugates

Borja Moreira-Alvarez, Andrea L. Larraga-Urdaz, Ana Fuentes-Cervantes, María Luisa Fernandez-Sánchez, Jose M. Costa-Fernández **, Jorge Ruiz Encinar *

Department of Physical and Analytical Chemistry, University of Oviedo, Avda. Julián Clavería 8, Oviedo 33006, Spain

ARTICLE INFO

Handling Editor: Qun Fang

Keywords:
Asymmetric flow field-flow fractionation
Multiangle light scattering
Inductively coupled plasma-tandem mass spectrometry
Gold nanoparticles
microRNA

ABSTRACT

In-depth characterization of functionalized nanomaterials is still a remaining challenge in nanobioanalytical chemistry. In this work, we propose the online coupling of Asymmetric Flow Field-Flow Fractionation (AF4) with UV/Vis, Multiangle Light Scattering (MALS) and Inductively Coupled Plasma-Tandem Mass Spectrometry (ICP-MS/MS) detectors to carry out, in less than 10 min and directly in the functionalization reaction mixture, the complete characterization of gold nanoparticles (AuNPs) functionalized with oligonucleotides and surface-modified with polyethylene glycol (PEG). AF4 separation provided full separation of the bioconjugates from the original AuNPs while P/Au and S/Au ICP-MS/MS ratios in the bioconjugate fractographic peaks could be used to compute the corresponding stoichiometries, oligonucleotide/AuNP and PEG/AuNPs. MALS detection clearly showed the coexistence of two distinct nanoparticulated populations in the bioconjugation mixture, which were demonstrated to be different not only in size but in functionality as well. The major bioconjugate population showed lower hydrodynamic ratios (18 nm) with higher and steadier oligonucleotides/AuNPs (92) and PEG/AuNPs (2350) stoichiometries, in comparison to the minor abundant population (54 nm, 51 and 1877, respectively). Moreover, the ratio between the absorbance signals measured at 520 nm and 650 nm reflects a lower AuNP aggregation in the major (10.5) than in the minor (4.5) population. Results obtained prove the benefits of a detailed characterization to find out if subsequent purification of functionalized AuNP-oligonucleotides is required to design more efficiently their final bioanalytical application.

1. Introduction

MicroRNAs, also called miRNAs, are single-stranded nucleic acids of between 19 and 25 nucleotides. Unlike other nucleic acids, they do not encode proteins but simply regulate gene expression. When they hybridize to messenger RNA (mRNA) sequences, they cause inhibition or degradation of this miRNA, leading to a decrease in the protein level encoded by that gene/mRNA. Therefore, there is great interest in the detection and quantification of miRNA, as they are considered key in cellular mechanisms and potential biomarkers of various pathologies [1].

Although standardized methods exist for miRNA detection as quantitative polymerase chain reaction (qPCR) [2,3], the rise of nanotechnology has brought a faster alternative that does not require specialized equipment. Recent studies have shown that measurement of changes in the Localized Surface Plasmon Resonance due to the aggregation of AuNPs induced by the presence of miRNAs is one of the promising tools for miRNA quantification [4]. In this particular case, a set of water stable AuNPs are modified with two distinct DNA oligonucleotide strands, each of them partially complementary at each end of the miRNA sequence of interest (target biomolecule). The presence of the target miRNA triggers its hybridization with the two types of functionalized AuNPs leading to aggregation that brings about a change that can be visually detected, from the red they show when are free AuNPs to the violet they show when aggregated [5]. Additionally several ligands, such as polyethylene glycol, are typically used to modify the surface of the AuNPs by blocking any DNA-free areas to minimize unspecific adsorptions and make them more biocompatible.

* Corresponding author. ,
** Corresponding author.
E-mail addresses: jcostafe@uniovi.es (J.M. Costa-Fernández), ruizjorge@uniovi.es (J.R. Encinar).

https://doi.org/10.1016/j.talanta.2023.124309
Received 23 December 2022; Received in revised form 23 January 2023; Accepted 25 January 2023
Available online 26 January 2023

In this type of colorimetric assays, the magnitude of the observed optical changes critically depends on the extent of the modification of the AuNPs surface with oligonucleotides and on the capability of complementary target oligonucleotides to access the surface-bound oligonucleotides. This explains the great deal of effort carried out toward development of methodologies capable to compute the surface coverage of DNA oligonucleotides bioconjugated onto Au nanoparticles. Knowledge about the type and number of DNA strands bound to the nanoparticle surface is essential to optimize the reproducibility, sensitivity, stability and efficiency of the assays [6,7].

The conventionally used fluorescence "turn-on" method measures the emission intensity of a fluorescent dye-labelled DNA [8], previously attached to the AuNP, after being displaced by small thiol ligands. This method requires assuming that all DNA ligands are completely displaced from the surface of the DNA–NPs. However, the rate and extent of thiol/ligand exchange depends strongly on the ligand identity, thus invalidating the previous assumption and resulting in errors in the determination. "Turn-off" fluorescent methods have been also proposed [9]. Here, the luminescence emission of a fluorophore-labelled DNA solution is measured before and after binding to the AuNPs. Measurement of the decrease in fluorescence caused by the AuNPs acting as a luminescence quencher is used for quantifying the DNA linked to the NPs. This approach assume that the fluorophore tag of the DNA is completely quenched upon binding with the AuNPs. However, the degree of deactivation depends on several factors, such as the quencher-fluorophore distance, which finally affect the quantification. Additionally, both fluorescent methods rely on the use of fluorophore labels that could affect DNA–NP ligand structure, reactivity, and in turns, the number of recognition strands bound to each AuNP, thus affecting the accuracy on the NP surface coverage determination [10].

Label-free DNA sequences attached to AuNPs have been quantified by subtracting the UV–Vis signal obtained in the supernatant before and after the bioconjugation reaction [11]. Although it is a very simple indirect method, it requires large amount of bioconjugates, and it cannot discriminate between oligonucleotides attached at the surface and the possible aggregated chains.

Some other analytical methods able to determine the number of DNA strands per AuNP without using fluorophores or making assumptions regarding nanoparticle reactivity have been proposed. A commonly used methodology involves the quantification of the electrophoretic movement of different bioconjugates to obtain a semi-quantitative information [6]. This approach is limited by the resolution power of the electrophoretic separation. It also presents the disadvantage of low recoveries due to losses or adsorptions produced along the numerous purification steps especially when the binding of biomolecules to NPs is not strong enough. Analysis of the total phosphorus content of the bioconjugate has been also used to relate this concentration to that of the oligonucleotide chains. This approach requires an efficient purification step to isolate the bioconjugate from the matrix components and perform digestion of the samples, which could entail contamination problems. Moreover, it only provides average oligonucleotide:AuNP stoichiometries with no information about the eventual presence of different bioconjugate populations in the sample [12].

Therefore, there is a strong demand of new robust methods able to accurately quantify the number of oligonucleotides per AuNP in the bioconjugates and also to identify the eventual presence of bioconjugated nanoparticulated species with different stoichiometries coexisting in a given sample [13]. Herein, we propose the use of an analytical platform based on the coupling of an Asymmetric Flow Field-Flow Fractionation (AF4) separation technique to different optical (UV/Vis absorbance and Multiangle Light Scattering) and elemental (inductively coupled plasma mass spectrometry, ICP-MS) detectors for the direct and integrated characterization of functionalized AuNP nanostructures especially designed for miRNA optical quantification. This study was aimed at gaining a key information for the prepared nanoparticle-oligonucleotide bioconjugate materials, including not only the average AuNP-ligands-complementary strands stoichiometries but also the assessment of eventual individual nanoparticulated populations eventually coexisting in the bioconjugate mixture.

2. Materials and methods

2.1. Reagents and materials

Hydrogen Tetrachloroaurate Trihydrate ($HAuCl_4 \cdot 3H_2O$), Sodium citrate tribasic dihydrate ($Na_3C_6H_5O_7 \cdot 2H_2O$), Magnesium Chloride Hexahydrate ($MgCl_2 \cdot 6H_2O$), Trizma® Hydrochloride ($NH_2C(CH_2OH)_3 \cdot HCl$), Potassium Chloride (KCl) and Tween20 were purchased from Sigma-Aldrich (Schnelldorf, Germany) while Thiolated Polyethylene Glycol (mPEG-SH1000) was purchased from Laysan Bio, Inc. (Huntsville, USA).

The oligonucleotides chains, with the thiol group protected, employed in the functionalization of the AuNPs were purchased from Integrated DNA Technologies (Iowa, USA).

2.2. Preparation of functionalized AuNPs

Two sets of the same AuNPs were functionalized with two distinct oligonucleotides chains via the high affinity of their thiol groups with the Au atoms at the NP surface. Two oligonucleotrides:AuNPs bioconjugates, named AuNPs-1 and AuNPs-2, were formed by coating the surface of the AuNPs with two nucleic acid chains «′-/5ThiolMC6-D/ AAA AAA AAA ACC TAT CGA CCA TGC T -3′» and «5′- CCG CTA GAG TCG TTT AAA AAA AAA A/3ThiolMC3-D -3′», respectively, which are partially complementary to a selected target Nucleic Acid species used for the specific detection of the miRNA 146a biomarker of mastitis.

The AuNPs were synthetized in out laboratory using the sodium citrate reduction method described in the literature (see the Supporting Information) [14]. The NP-surface functionalization process consists of several steps. In a first step, the oligonucleotide strands were deprotected to leave the thiol accessible. For this purpose, 20 μL of 10 μmol/L of the blocked strand and 108 μL of 1.8 mmol/L tris(2-carboxyethyl) phosphine (TCEP) were incubated for 2 h at room temperature in a 90 mmol/L solution of trisodium citrate HCl buffer (pH 3) with 0.01% v/v Tween20. The surface of the AuNPs was coated with such unprotected oligonucleotides by incubating them for 20 min at room temperature with the desired concentration of AuNPs.

The remaining free surface of the already functionalized AuNPs was then coated to further stabilize the nanostructures and minimize possible non-specific interactions. For this purpose, the AuNPs-1 and AuNPs-2 were incubated for 30 min at 60 °C with 40 μL of 2 mmol/L thiolated polyethylene glycol 1 kDa (mPEG). Once AuNPs were stabilized, a multiple purification steps through centrifugations at 8000 g for 30 min at 4 °C were performed for removal of the excess of unreacted reagents. Finally, functionalized AuNPs were redispersed in ultrapure water with 0.01% v/v Tween-20, resulting in a concentration of 10 nM in AuNPs (quantified by UV/Vis) and stored at 4 °C until further use.

2.3. Instrumentation

UV/Vis absorbance was recorded on Genesys 10S spectrophotometer (Thermo Scientific, Germany) using conventional quartz SUPRASIL cuvettes (Hellma Analytics, Germany). Measurement of the hydrodynamic radius of the nanoparticles and their Z-potential determination were carried out with DLS Zetasizer Nano ZS (Malvern, United Kingdom).

The Asymmetric Flow Field-Flow Fractionation (AF4) system used was an AF2000 MT instrument (Postnova Analytics, Germany). The channel was formed by a polyethersulfone (PES) membrane with 10 kDa cut-off (changed every ca. 25 injections) and a 500 μm spacer. The optimized flow rate program employed for nanoparticle separation is summarized in Table S1. 0.05% Tween80® in MilliQ double filtered by 0.1 μm PVDF filters was used as carrier solution. The AF4 system was

coupled online to an UV/Vis absorbance detector Agilent 1260 Infinity MWD (Agilent, Germany); a Multiangle light scattering MALS PN3621 (Postnova Analytics Inc., Germany); and an ICP-MS/MS instrument (Agilent 8900, Japan). Operation conditions of all the detectors are summarized in Table S2. Integration of the fractographic peaks was performed using the MassHunter software (Agilent). Sample recovery was calculated comparing the sum of the Au peak areas obtained during the AF4 separation with that obtained without cross flow (FIA).

Oxygen was introduced in the reaction cell of the ICP-MS/MS instrument at a flow of 0.35 mL min−1. In order to detect S and P free of interferences in mass shift MS/MS mode ($^{32}S^+ \rightarrow {}^{48}SO^+$ and $^{31}P^+ \rightarrow {}^{47}PO^+$, respectively) [15]. Although Au was not interfered and the Au oxide formation rate at the cell was extremely low, we still selected mass shift mode for Au detection ($^{197}Au^+ \rightarrow {}^{213}AuO^+$) in order to detect gold in digital mode as well, together with P and S oxides, and not saturate the SEM detector (NP core was made exclusively of Au atoms).

3. Results and discussion

3.1. Characterization of the free AuNPs

The first step for the in-depth characterization of the desired functionalized bioconjugates was to study the naked AuNPs synthesized in our laboratory. Although the synthetic methodology follows a well-known controlled process, there could be still some experimental variability of the NPs generated in terms of the size, size-dispersion and aqueous stability. These variations may lead to unsuitable AuNPs bioconjugates products that may affect the bioassay at a later stage. Here transmission electron microscopy (TEM) was used to measure the NP size and morphology. The hydrodynamic radius and the polydispersity index (PDI) of AuNPs were measured using dynamic light scattering (DLS). AuNPs with sizes around 15 nm and PDI smaller than 0.1 were synthesized and used for bioconjugation to the DNA oligomers. The results obtained shown in Fig. S1. Hydrodynamic diameter of 19.4 nm and a PDI of 0.07 are consistent with those obtained by TEM measurements (15 ± 1 nm, Fig. S2).

After simple dilution of the solution resulting from the AuNPs synthesis with 0.01% Tween20, an aliquot of the diluted sample was injected into the platform AF4-UV/Vis-MALS-ICP-MS/MS (Fig. S3a). Experimental conditions were previously optimized to obtain the highest possible recovery of the target bioconjugates while providing their complete separation from the free unreacted AuNPs (Table S1). The low NPs recovery obtained with respect to the FIA signal (62%) and the significant tailing of the peak seemed to pinpoint towards the low stability of the free AuNPs in the system under such separation conditions. The results obtained by MALS (Fig. S3b) for the main peak (6.5–8 min) showed that 80% of the NP detected therein reached large size (54 ± 5 nm, radius), with clear evidence of less abundant and even bigger populations which suggest that AuNPs are aggregated under these conditions. The Zeta potential result obtained, −7.83 ± 4.21 eV (Fig. S1b), corroborated the AuNPs instability. It should be noted that such instability of the free AuNPs was observed due to the AF4 compromise conditions (0.01% Tween20) used, because our purpose was to know the behavior and elution profile of unreacted AuNPs likely still present in the resulting bioconjugation mixtures of our targets, AuNPs-1 and AuNPs-2.

3.2. Characterization of oligonucleotides:AuNP bioconjugates

AuNPs were functionalized with two distinct oligonucleotide strands following the procedure described above. As mentioned in the introduction, novel miRNA quantification assays are based on the analyte-induced aggregation of functionalized AuNPs producing detectable changes in the Surface Plasmon Resonance (SPR) absorption wavelengths of the NPs. For this purpose, AuNPs are modified with short oligonucleotide sequences, which are partially complementary to the target sequence. Here, the proposed analytical platform will be assayed to optimize bioconjugation and perform adequate characterization of the two oligonucleotide-functionalized AuNPs species that will be used in the design of a colorimetric method for the detection of miRNA.

Eight oligonucleotide:AuNP molar ratios were tested ranging from 0:1 to 250:1. In all cases, the resulting bioconjugate mixture was incubated with an excess of the thiolated-mPEG ligand to reduce unspecific interactions by coating the remaining oligonucleotide-free AuNP surface. The characterization of the samples was performed first off-line using conventional methods and then employing the proposed AF4-UV/Vis-MALS-ICP-MS/MS platform.

3.2.1. Off-line characterization of bioconjugates

Gel electrophoresis is widely used for characterization of biomolecule:nanoparticle bioconjugates [16]. In the particular case of the oligonucleotide-AuNPs here synthesized, all the functionalized nanoparticles were further coated with mPEG. Thus the differences in species mobility depended exclusively on the surface charge, which was in turn function of the number of the oligonucleotide strands initially bioconjugated. The different functionalized AuNPs were first characterized using gel electrophoresis following the procedure described in the Supporting Information. The images of the gels obtained for both bioconjugates (AuNPs-1 and AuNPs-2) prepared under the different oligonucleotide:AuNPs molar ratios assayed are shown in Fig. S4. Although the two oligonucleotide chains have the same number of phosphates and therefore the same number of negative charges, the behavior of the two bioconjugates was slightly different. In both cases the bioconjugated blank, which consisted of coating the AuNPs simply with mPEG, hardly advanced through the gel because the mPEG does not provide any charge to the AuNPs.

In the case of AuNPs-1 (Fig. S4a), the nanostructures prepared using 10:1 and 25:1 oligonucleotide:AuNPs molar ratios showed broad diffuse bands, that might be because of heterogeneity problems in the biomolecule coating of the AuNPS. The functionalized nanoparticle prepared using the 50:1 oligonucleotide:AuNPs molar ratio, although still produced a slight broad band, it was much narrower than the previous ones. Functionalized AuNPs prepared using higher amounts of oligonucleotides produced gel bands that were significantly narrower appearing approximately at the same distance in the gel independent on the oligonucleotide:AuNPs molar ratio used in the preparation. This seems to indicate that the differences between charges in the prepared bioconjugates were minimal because the oligonucleotide surface coverage level in the AuNPs reached a plateau. In contrast, the AuNPs-2 bioconjugate (Fig. S4b) showed broad bands only at 10:1 and 25:1 M ratios, reaching the stabilization already at ratio 50:1 oligonucleotide:AuNPs.

Z-potential measurements were also performed to confirm that the aggregation of the samples was due to insufficient electrostatic charge on some of the oligonucleotide:AuNP ratios assayed. In fact, as the number of strands present in the different bioconjugates increased, the absolute values of the Z-potential raised (−16.4 ± 6.0; −25.4 ± 4.5 eV; −28.6 ± 7.9 and −29.8 ± 6.5 eV for 10:1, 25:1, 150:1 and 250:1 respectively) towards the threshold value of −30 eV (where they are considered to have a stable charge) [17].

3.2.2. Bioconjugate characterization by AF4-UV/Vis-MALS-ICP-MS/MS platform

In parallel, the bioconjugate mixtures prepared using different oligonucleotide:AuNP ratios were analysed using the AF4-UV/Vis-MALS-ICP-MS/MS analytical platform. First of all, it is worth noting that AF4 recoveries using PES membrane (85 ± 5%) were much higher than that found for the analysis of the free AuNPs, and peaks obtained were Gaussian and relatively narrow reaching baseline in less than 2 min. Notably, the use of regenerated cellulose membranes led to much lower recoveries for such bioconjugate mixtures (57 ± 6%). As an example, the signals obtained by the different detectors for the 100:1 oligonucleotide:AuNPs ratio assayed in bioconjugates AuNPs-1 and

AuNPs-2 are shown in Fig. 1. The complete set of fractograms corresponding to the rest of bioconjugate ratios are given in Figs. S5–S10. Similarly to the gel electrophoresis results, the fractograms obtained became stable as the oligonucleotide:AuNP ratios increased over 50:1 oligonucleotide:AuNPs, with a major species eluting at the same time, 4.8 min for both, the AuNPs-1 and the AuNPs-2. Additionally, a minor species could also be detected later as a peak shoulder at 5.4 min.

One power of the analytical platform presented herein is the complementary information obtained from the different detectors used, that is of paramount value for unequivocal identification of the nanoparticulated species separated during the AF4 analysis. As shown in Fig. 1, MALS signals at 90° could clearly differentiate two populations within the bioconjugate peak that were hardly detected as small shoulders with the other two detectors. Analysis of such complementary information allowed us to find out that both peaks corresponded to the same nanoparticulated species with a slightly different aggregation level. Nanoparticle aggregation did not involve any significant change in the elemental (Au, S, P) contents or the wavelength signals provided by the ICP-MS/MS and the UV/Vis detectors, respectively, but it brought about a significant conformation change easily detectable by MALS. In fact, it is remarkable that the longer elution time of the minor bioconjugate population in Fig. 1 (around 5.4 min in AuNPs-1 and AuNPs-2 and shaded in blue), likely corresponding to aggregates as previously discussed, is relatively close to the elution time observed for the free AuNPs (6.4 min, see Fig. S3a) that were already demonstrated to be highly aggregated. As can be observed in the collection of MALS signals obtained for four different oligonucleotide:AuNP ratios in AuNPs-1 in Fig. 2a, this minor, later eluting and likely aggregated bioconjugate population was the major one in the 10:1 ratio (with even longer elution time, 5.7 min) and still very significant in the 25:1ratio. It seems evident that the stabilization provided by the adequate covering with the oligonucleotide strands attached to the surface prevented aggregation. This protective effect results in a major bioconjugate species eluting in the first "non-aggregated region" (shaded in yellow in Figs. 1 and 2) when the oligonucleotide:AuNPs ratio is above 50:1. A similar behavior with shorter elution times as the oligonucleotide:AuNP ratio increased, was also apparent in the Au signals from the ICP-MS/MS given in Fig. 2b for the same ratios.

3.2.2.1. Hydrodynamic radius (MALS) determination of bioconjugates. After treatment of the fractograms signals obtained measuring the light scattered at the 21 angles on-line monitored with the MALS detector, we could obtain the hydrodynamic size of the different NP populations separated using the AF4 system. The results obtained for the analysis of the different oligonucleotide:AuNPs ratios assayed are given in Table 2. It is well-known that oligonucleotide strands smaller than 30 bases are stretched and well-packed, so the size of the resulting bioconjugate nanostructure could be roughly estimated as the sum of the diameter of the original AuNP core plus twice the strand size [18]. Considering that the AuNP core was 15 nm diameter (average value measured by TEM) and each of the bases of the 25-nucleotide strand has 0.4 nm, the theoretical size expected for the bioconjugates will be around 35 nm diameter (17.5 nm in radius). As can be seen in Table 2, the hydrodynamic radius of the first major population (shaded in yellow in Figs. 1

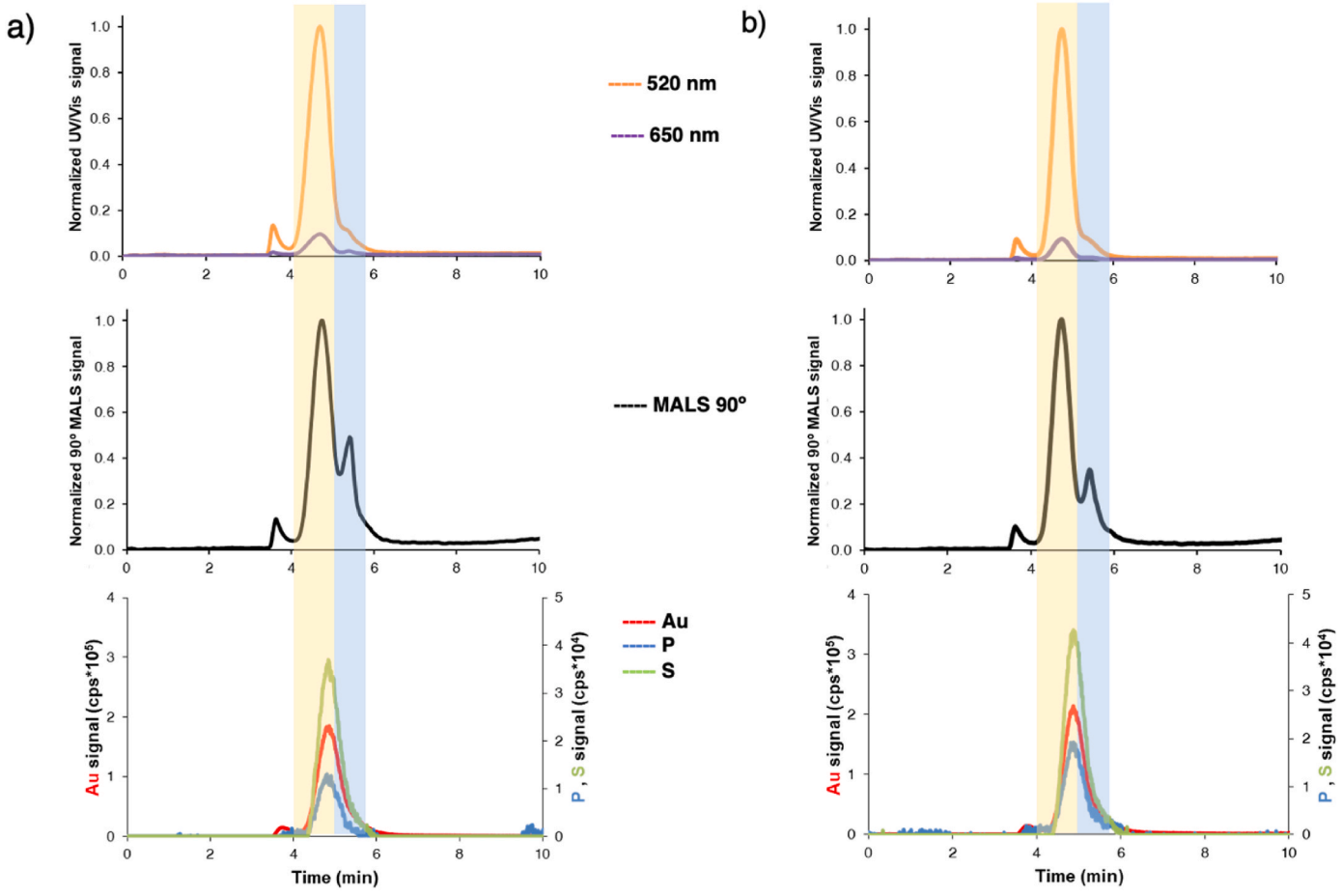

Fig. 1. AF4-UV/Vis-MALS-ICP-MS/MS analysis of the bioconjugate mixtures using the 100:1ratio (oligonucleotide:AuNPs). (a) Fractograms from the analysis of the AuNPs-1, (b) fractograms from the analysis of the AuNPs-2. The peaks corresponding to the first (non-aggregated) and the second (aggregated) bioconjugate populations, as clearly indicated by MALS signals, are shaded in yellow and blue respectively. (For interpretation of the references to color in this figure legend, the reader is referred to the Web version of this article.)

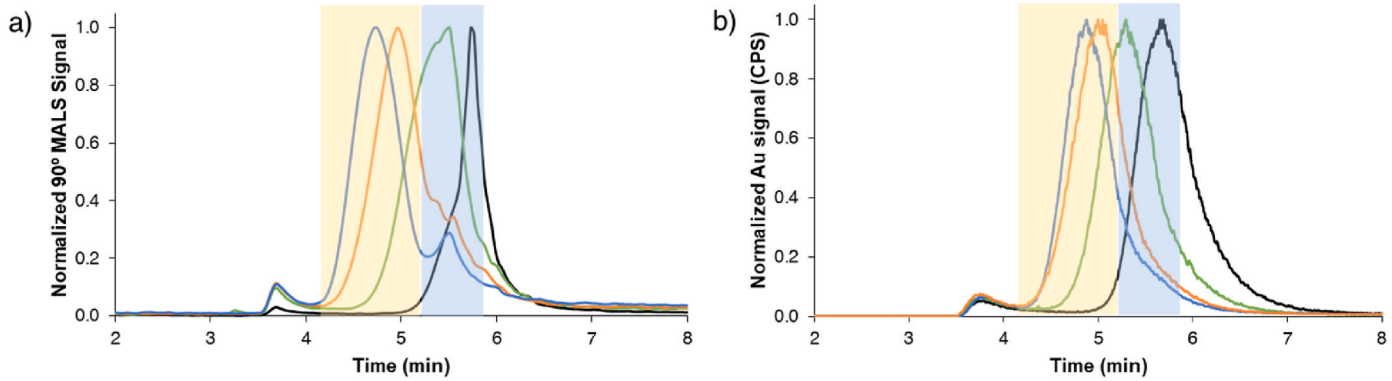

Fig. 2. Comparison of the fractograms obtained for the analysis of the AuNPs-1 bioconjugate prepared using different molar ratios oligonucleotide:AuNPs: 10:1 (black), 25:1 (green), 50:1 (orange) and 150:1 (blue). a) MALS signal, b) Au signal obtained by the ICP-MS/MS. The fractogram regions corresponding to the first (non-aggregated) and to the second (aggregated) bioconjugate populations are shadowed in yellow and blue, respectively. (For interpretation of the references to color in this figure legend, the reader is referred to the Web version of this article.)

and 2) stabilized around 19 nm for the MALS analysis of AuNPs-1 bioconjugates prepared using oligonucleotide:AuNPs ratios of 50:1 and above and ratios over 25:1 for AuNPs-2 bioconjugates, which is fully consistent with the theoretical expected size. These hydrodynamic results supported the assumption that the first eluting species corresponded to non-aggregated AuNPs functionalized with the oligonucleotides (both 1 and 2). Hydrodynamic sizes for the first population at 10:1 ratio assayed could not be computed as no peak was obtained. Hydrodynamic sizes for the first population at 25:1 and 50:1 (Figs. S6 and S7, respectively) were slightly higher because the AF4 separation from the second aggregated population was not complete.

Table 1 also shows that the hydrodynamic size obtained using online MALS for the second fractographic population, shaded in blue in Figs. 1 and 2, was always significantly bigger (around 54 and 45 nm for analysis of the bioconjugate mixtures of AuNPs-1 and AuNPs-2, respectively) and very close to that obtained for the most abundant population observed in the free (and aggregated) AuNPs (54 ± 5 nm). Two hypotheses might be stated from these results. Either bioconjugation was not complete (specially at the lower ratios assayed) and this second population corresponds to unreacted and aggregated AuNPs or bioconjugate species produced at low oligonucleotide:AuNP ratios were not stable enough and were prone to aggregate along the bioconjugation reaction process. Notably, although MALS signal allowed us to distinguish clearly the presence of two populations in the AF4 fractograms, it was not sufficient to provide complete information about their nature.

Table 1
Hydrodynamic radius obtained using AF4-MALS for the first and second bioconjugate populations shaded yellow and blue respectively in Figs. 1 and 2 for the different oligonucleotide:AuNP ratios assayed. Uncertainty corresponds to one standard deviation (n = 3).

	First Population		Second Population	
Ratio assayed oligonucleotide:AuNP	AuNPs-1	AuNPs-2	AuNPs-1	AuNPs-2
AuNPs	–	–	54.2 ± 5.4	54.2 ± 5.4
10:1	–	–	42.2 ± 4.2	36.2 ± 3.6
25:1	27.2 ± 2.7	21.8 ± 2.2	55.8 ± 5.6	43.0 ± 4.3
50:1	21.6 ± 2.2	19.4 ± 1.9	54.8 ± 5.5	44.6 ± 4.5
100:1	19.0 ± 1.9	17.6 ± 1.8	53.0 ± 5.3	44.2 ± 4.4
150:1	18.4 ± 1.8	19.2 ± 1.9	55.4 ± 5.5	45.2 ± 4.5
200:1	18.6 ± 1.9	20.8 ± 2.1	53.6 ± 5.4	46.8 ± 4.7
250:1	19.6 ± 2.0	18.8 ± 1.9	54.2 ± 5.4	45.0 ± 4.5

Table 2
520–650 nm intensity ratios obtained using AF4-UV/vis for the first and second populations for the different oligonucleotide:AuNP ratios assayed. Uncertainty corresponds to one standard deviation (n = 3).

	First Population		Second Population	
Ratio assayed oligonucleotide:AuNP	AuNPs-1	AuNPs-2	AuNPs-1	AuNPs-2
AuNPs	–	–	7.0 ± 1.2	8.3 ± 1.7
10:1	10.5 ± 0.2	10.5 ± 0.1	5.5 ± 0.3	4.7 ± 0.3
25:1	10.4 ± 0.1	10.4 ± 0.1	5.1 ± 0.4	3.9 ± 0.4
50:1	10.4 ± 0.1	10.5 ± 0.1	4.3 ± 0.3	4.1 ± 0.3
100:1	10.6 ± 0.1	10.6 ± 0.1	5.8 ± 0.3	4.7 ± 0.2
150:1	10.2 ± 0.1	10.7 ± 0.1	4.0 ± 0.4	4.7 ± 0.2
200:1	10.5 ± 0.1	10.2 ± 0.1	5.1 ± 0.4	3.2 ± 0.4
250:1	10.5 ± 0.1	10.2 ± 0.1	5.1 ± 0.4	3.2 ± 0.4

3.2.2.2. UV/Vis behavior: aggregation studies. A simple and well-known way to study the aggregation of AuNPs is to detect changes on the UV–Vis spectrum of the sample containing the nanoparticles. For AuNPs of about 15 nm diameter size the absorbance ratios measured at the maximum wavelength of the LSPR of free AuNPs (520 nm) and at a second wavelength at which isolated AuNPs do not absorb but aggregated (e.g. 650 nm) is a useful parameter to estimate the degree of NPs aggregates in the sample [19]. In absolute terms, the lower the ratio, the more aggregated the gold nanostructures are.

Based on such ratiometric approach UV/Vis detection coupled to the AF4 separation was investigated as a tool to study the eventual aggregation state in the different populations. The data for the two populations separated in the AF4 for the analysis of the bioconjugates preparated at the different oligonucleotide:AuNPs ratios assayed are shown in Table 2. Such results corroborated that the second nanoparticulated population contains a much higher degree of AuNP aggregated (higher Abs650/Abs520) as compared to the first fractionated population.

3.2.2.3. Determination of the stoichiometry oligonucleotide:AuNP using ICP-MS/MS. ICP-MS and the determination of metal to sulfur ratios has been already reported as a viable alternative for the characterization of NP, the quantification of the ligand density on their surface and the estimation of protein corona content [20–22]. This exceptional feature becomes even more powerful when the ICP-MS is coupled on-line to CE [23] and especially to AF4 separations as it opens the door to the elemental characterization of the individual nanostructure populations present in bioconjugation reaction mixtures [24].

In this case, the coupling of a tandem ICP-MS detector (ICP-MS/MS) to the AF4 separation allowed to quantify simultaneously both the low P and S signals coming from the oligonucleotide and PEG molecules attached to the NP surface and the high intensity signal of Au from the NP core. Such information was crucial to characterize further the nanoparticulated species coexisting in the bioconjugation mixtures. Previously, the number of Au atoms present per NPs was determined by direct ICP-MS/MS analysis of the acid-digested NPs solution. Both Au and NPs concentrations (calculated by PCA analysis) and their corresponding uncertainties were then related. The resulting Au atoms per NP obtained was 104,275 ± 6256 (1 SD, n = 5). On the other hand, the number of phosphate groups per oligonucleotide (1 and 2) bioconjugated is known.

The methodology for the determination of the molar oligonucleotide:AuNP stoichiometry is based on the one previously developed by Bouzas et al. [25] for the determination of the molar antibody:QD stoichiometry and it is illustrated in Fig. 3. Briefly, it relies on the P:Au intensity ratio determination in the corresponding AF4-ICP-MS/MS bioconjugate peaks present in the two shaded regions in Figs. 1 and 2. Such mean intensity ratios (at least of 50 different points) for the bioconjugate populations could be then translated into P:Au molar ratios using external FI calibration (Fig. S11) built using generic Au and P inorganic standards since elemental signals provided by ICP-MS/MS are virtually species independent. Such molar ratios together with the number of P atoms in the oligonucleotide strands and the number of Au atoms per AuNP were combined to obtain the individual oligonucleotide:AuNP stoichiometries (see Table 3) for the aggregated and non-aggregated populations (blue and yellow shaded regions in Figs. 1 and 2) in each oligonucleotide:AuNP (AuNPs-1 and AuNPs-2) mixture ratio assayed. P signal for the bioconjugate peak obtained using a 10:1 oligonucleotide:AuNPS ratio was so small that any stoichiometry could be obtained in this case (Fig. S5). The oligonucleotide:AuNP stoichiometry obtained for the first eluting non-aggregated yellow-shaded population steadily increased with the oligonucleotide:AuNP ratio assayed up to 75 ± 7 and 109 ± 9 for the AuNPs-1 and AuNPs-2, respectively. This is likely because the strand-2 is better packed than strand-1 leading to higher ligand density over the same AuNP. To the best of our knowledge, this is the first time that the number of oligonucleotide strands bioconjugated on the surface of AuNPs (stoichiometry) could be computed directly in a single analysis and without any sample preparation.

In contrast, the oligonucleotide:AuNP stoichiometry values obtained for the second blue-shaded population did not show any clear trend and showed higher variability between replicates (precision ranged between 16 and 53% RSD). This is again clear evidence that the species eluted at this time correspond to aggregates with high variability in the structure/composition.

Table 3
Oligonucleotide:AuNP stoichiometries obtained using AF4-ICP-MS/MS for the two bioconjugate populations shaded in Figs. 1 and 2. Combined uncertainty corresponds to one standard deviation (n = 2). Values for free AuNPs and bioconjugates obtained at 10:1 ratio could not be computed because P signal was below the detection limit.

	First Population		Second Population	
Ratio assayed oligonucleotide: AuNP	AuNPs-1	AuNPs-2	AuNPs-1	AuNPs-2
AuNPs	–	–	–	–
10:1	–	–	–	–
25:1	28 ± 4	25 ± 3	46 ± 15	32 ± 17
50:1	37 ± 4	54 ± 5	27 ± 7	51 ± 13
100:1	48 ± 5	77 ± 7	31 ± 11	87 ± 14
150:1	65 ± 6	84 ± 8	68 ± 11	47 ± 17
200:1	67 ± 6	99 ± 8	38 ± 15	62 ± 13
250:1	75 ± 7	109 ± 9	51 ± 10	58 ± 19

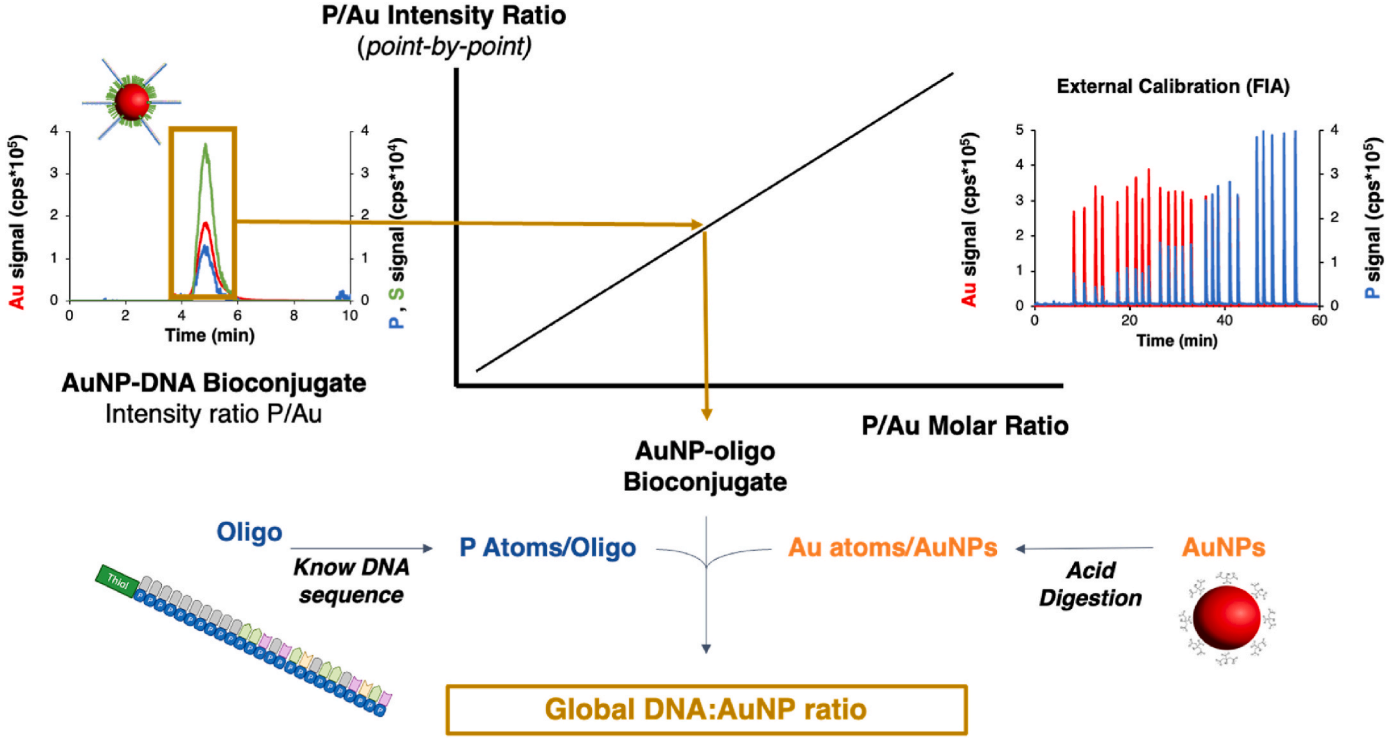

Fig. 3. Workflow employed for the determination of the oligonucleotide:AuNP stoichiometries in the different bioconjugate mixtures analysed.

3.2.2.4. Overall ligand density computation using ICP-MS/MS. Both the thiolated-oligonucleotides used first for functionalization and the thiolated-PEG used afterwards to avoid unspecific interactions have one S atom per molecule and are strongly attached to the Au surface. Therefore, by accurately quantifying the S:Au molar ratio using the data provided by the ICP-MS/MS detector we could assess the total number of biomolecules (including oligonucleotide and PEG) that each of the bioconjugate populations have attached over their surface. Again, we measured the point-by-point S:Au intensity ratio along the bioconjugate peaks present in the two shaded regions. The mean of the intensity ratios for each bioconjugate populations could be then translated into S:Au molar ratios using again external FI calibration and generic S and Au inorganic standards (Fig. S12). Such molar ratios together with the number of S atoms per ligand molecule and the number of Au atoms per AuNP were combined to obtain the individual ligand:AuNP stoichiometries for the aggregated and non-aggregated populations (blue and yellow shaded regions in Figs. 1 and 2) in each oligonucleotide:AuNP (AuNPs-1 and AuNPs-2) ratio assayed (10:1–250:1). The results obtained shown in Table 4 indicated that the number of anchor points of the first population (once it could be detected) was constant with an average value of 2376 ± 150 S/AuNPs for the bioconjugate AuNPs-1 and 2335 ± 120 S/AuNPs for the bioconjugate AuNPs-2. The global coating finally obtained on this first population was then very uniform, independently of the initial surface coverage with oligonucleotides. Therefore it is evident that the reason to obtain lower oligonucleotide:AuNP stoichiometries (75 and 109 for AuNPs-1 and AuNPs-2) than those assayed (250, as seen in Table 3) was not the lack of free space in the AuNP surface but the electrostatic repulsions between the high negatively-charged oligonucleotides. This finding seems to indicate as well that the oligonucleotides were homogeneously placed over the AuNPs surface.

In the case of the second population, and similarly to that shown in Table 3 with the oligonucleotide:AuNP stoichiometries, the overall coating obtained was again significantly lower than that obtained for the first population with higher variability. Considering all information obtained for the second population using the individual detectors (Tables 1–4), we can conclude that this nanoparticulate species was a by-product of the bioconjugation reaction consisting mainly of aggregates. Such aggregation, that took place during incubation with the oligonucleotide strands led to a reduction in the surface area available for both oligonucleotide and PEG coating. Of course, the oligonucleotide and global ligand density attainable depended on the aggregation-interaction in each case and therefore it became very variable.

Table 4
Overall oligonucleotide:AuNP stoichiometries obtained in the two AF4 populations shaded in Figs. 1 and 2. Combined uncertainty corresponds to one standard deviation (n = 2).

	First Population		Second Population	
Ratio assayed oligonucleotide:AuNP	AuNPs-1	AuNPs-2	AuNPs-1	AuNPs-2
AuNPs	–	–	2441 ± 224	2441 ± 224
10:1	–	–	2113 ± 173	2136 ± 188
25:1	2600 ± 215	2454 ± 194	1742 ± 344	2519 ± 221
50:1	2489 ± 198	2383 ± 192	1754 ± 273	2103 ± 213
100:1	2380 ± 188	2388 ± 188	1873 ± 172	1762 ± 251
150:1	2440 ± 193	2292 ± 186	1250 ± 258	1956 ± 199
200:1	2340 ± 191	2214 ± 177	1131 ± 211	1339 ± 239
250:1	2271 ± 183	2480 ± 200	— (high S background)	1438 ± 236

4. Conclusions

This work has demonstrated the great versatility of the proposed AF4-MALS-ICP-MS/MS analytical platform for the comprehensive characterization and optimization of oligonucleotide-functionalized gold nanostructures for their later use in bioanalytical applications.

The combination of the great separation capabilities of AF4 for functionalized nanostructures (sample recovery of 85%) with the complete set of complementary (size, optical and elemental) information provided by the different detectors allows, in a single direct analysis (10 min), not only to find out whether the NP functionalization has been successful but also to characterize the individual bioconjugate populations formed under the different reaction conditions assayed. In fact, the integrated and multidisciplinary information obtained allowed to find out the presence of a minor non-stable bioconjugate species even at high oligonucleotide:AuNP molar ratios assayed that could not be detected by a conventional gel electrophoresis analysis or by Z-potential off-line measurements. It is important to stress here that although the MALS signal allowed to clearly distinguish the presence of this minor second population (aggregated and not stable) in the bioconjugation mixture, it did not provide at all structural information or the relative abundance of each population since the MALS signal is extremely size dependent. However, the quantitative and species-independent response in ICP-MS/MS (Au signal) provides additional estimation of the relative abundance of the different coexisting nanoparticulated species.

The integrated platform proposed is a powerful diagnostic tool in the quality control production of different complex nanostructures potentially used in immunoassays and imaging-trafficking studies. Notably, once different populations are identified in the resulting reaction mixture, fractions can be collected to obtain solutions containing highly pure functionalized NP with optimum features (size, stability, stoichiometry, optical properties). The approach here proposed is general and could be applied to any other type of inorganic NP (e.g., Ag, Pt, Cu) functionalized with any type of biomolecule with the only requisite that they contain P (nucleic acid material) or S (ligands, proteins) that could be measured by ICP-MS/MS. Additionally, it is not constrained by the type of interaction created between the NP and the ligand, no matter whether it is controlled by chemical (e.g. EDC chemistry), affinity (e.g. biotin-avidin) or physical (surface adsorption) interactions.

Credit author statement

Borja Moreira-Alvarez: Writing- Original draft preparation, Investigation, Methodology, Data treatment Andrea L Larraga-Urdaz: Investigation, Methodology. Ana Fuentes Cervantes: Methodology M.L. Fernandez-Sanchez: Supervision. Jose M Costa-Fernandez: Conceptualization, Writing- Reviewing and Editing, Supervision. Funding acquisition Jorge Ruiz Encinar: Conceptualization, Writing- Reviewing and Editing, Supervision, Funding acquisition.

Declaration of competing interest

The authors declare no financial interests/personal relationships which may be considered as potential competing interests.

Data availability

Data will be made available on request.

Acknowledgements

This work was supported by Spanish Ministry of Science and Innovation (PID2019-109698 GB-I00) and the Principality of Asturias GRUPIN IDI 2021/000081. B.M.A and A.F.C. thank the Ministry of

Economy and Competitiveness for their grants (BES-2017-080893 and FPU2019/00006 respectively). A.L.L.U. thank Principality of Asturias for the Severo Ochoa grant (PA-21-PF- BP19-059). Authors also wish to thank Agilent Technologies for the technical support.

Appendix A. Supplementary data

Supplementary data to this article can be found online at https://doi.org/10.1016/j.talanta.2023.124309.

References

[1] C.E. Condrat, D.C. Thompson, M.G. Barbu, O.L. Bugnar, A. Boboc, D. Cretoiu, N. Suciu, S.M. Cretoiu, S.C. Voinea, miRNAs as biomarkers in disease: latest findings regarding their role in diagnosis and prognosis, Cells 9 (2020) 276, https://doi.org/10.3390/cells9020276.

[2] I. Balcells, S. Cirera, P.K. Busk, Specific and sensitive quantitative RT-PCR of miRNAs with DNA primers, BMC Biotechnol. 11 (2011) 70, https://doi.org/10.1186/1472-6750-11-70.

[3] S. Khoury, N. Tran, qPCR multiplex detection of microRNA and messenger RNA in a single reaction, PeerJ 8 (2020), https://doi.org/10.7717/peerj.9004.

[4] R. Elghanian, J.J. Storhoff, R.C. Mucic, R.L. Letsinger, C.A. Mirkin, Selective colorimetric detection of polynucleotides based on the distance-dependent optical properties of gold nanoparticles, Science 277 (1997) 1078–1081, https://doi.org/10.1126/science.277.5329.1078.

[5] A. Sánchez Visedo, B. Gallego, L.J. Royo Martín, A.B. Soldado Cabezuelo, M. Valledor Llopis, F.J. Ferrero Martín, J.C. Campo Rodríguez, J.M. Costa Fernández, M.T. Fernández Fernández-Argüelles, Visual detection of microRNA146a by using RNA-functionalized gold nanoparticles, Microchim. Acta 187 (2020), https://doi.org/10.1007/s00604-020-4148-4.

[6] D. Zanchet, M. Micheel, W.J. Parak, D. Gerion, S.C. Williams, A.P. Alivisatos, Electrophoretic and structural studies of DNA-directed Au nanoparticle groupings, J. Phys. Chem. B 106 (2002) 11758–11763, https://doi.org/10.1021/jp026144c.

[7] A. Heuer-Jungemann, P.K. Harimech, T. Brown, A.G. Kanaras, Gold nanoparticles and fluorescently-labelled DNA as a platform for biological sensing, Nanoscale 5 (2013) 9503–9510, https://doi.org/10.1039/C3NR03707J.

[8] L.M. Demers, C.A. Mirkin, R.C. Mucic, R.A. Reynolds, R.L. Letsinger, R. Elghanian, G. Viswanadham, A fluorescence-based method for determining the surface coverage and hybridization efficiency of thiol-capped oligonucleotides bound to gold thin films and nanoparticles, Anal. Chem. 72 (2000) 5535–5541, https://doi.org/10.1021/ac0006627.

[9] X. Zhang, M.R. Servos, J. Liu, Instantaneous and quantitative functionalization of gold nanoparticles with thiolated DNA using a pH-assisted and surfactant-free route, J. Am. Chem. Soc. 164 (2012) 7266–7269, https://doi.org/10.1021/ja3014055.

[10] R.E. Paliwoda, F. Li, M.S. Reid, Y. Lin, X.C. Le, Sequential strand displacement beacon for detection of DNA coverage on functionalized gold nanoparticles, Anal. Chem. 86 (2014) 6138–6143, https://doi.org/10.1021/ac501341t.

[11] B.L. Baldock, J.E. Hutchison, UV–Visible spectroscopy-based quantification of unlabeled DNA bound to gold nanoparticles, Anal. Chem. 88 (2016) 12072–12080, https://doi.org/10.1021/acs.analchem.6b02640.

[12] J.A. Milton, S. Patole, H. Yin, Q. Xiao, T. Brown, T. Melvin, Efficient self-assembly of DNA-functionalized fluorophores and gold nanoparticles with DNA functionalized silicon surfaces: the effect of oligomer spacers, Nucleic Acids Res. 41 (2013) e8, https://doi.org/10.1093/nar/gkt031.

[13] B. Moreira-Alvarez, L. Cid-Barrio, H.S. Ferreira, J.M. Costa-Fernandez, J. R. Encinar, Integrated analytical platforms for the comprehensive characterization of bioconjugated inorganic nanomaterials aiming at biological applications, J. Anal. At. Spectrom. 8 (2020) 1518–1529, https://doi.org/10.1039/D0JA00147C.

[14] J.J. Storhoff, R. Elghanian, R.C. Muc, C.A. Mirkin, R.L. Letsinger, One-pot colorimetric differentiation of polynucleotides with single base imperfections using gold nanoparticle probes, J. Am. Chem. Soc. 120 (1998) 1959–1964, https://doi.org/10.1021/ja972332i.

[15] F. Calderón-Celis, N. Sugiyama, M. Yamanaka, T. Sakai, S. Diez-Fernández, J. J. Calvete, A. Sanz-Medel, J.R. Encinar, Enhanced universal quantification of biomolecules using element MS and generic standards: application to intact protein and phosphoprotein determination, Anal. Chem. 91 (2019) 1105–1112, https://doi.org/10.1021/acs.analchem.8b04731.

[16] P. Fagúndez, S. Botasini, J.P. Tosar, E. Méndez, Systematic process evaluation of the conjugation of proteins to gold nanoparticles, Heliyon 7 (2021), e07392, https://doi.org/10.1016/j.heliyon.2021.e07392.

[17] J.D. Clogston, A.K. Patri, Zeta potential measurement. In characterization of nanoparticles intended for drug delivery, Methods Mol. Biol. 697 (2011) 63–70, https://doi.org/10.1007/978-1-60327-198-1_6. PMID, 21116954.

[18] W.J. Parak, T. Pellegrino, C.M. Micheel, D. Gerion, S.C. Williams, A.P. Alivisatos, Conformation of oligonucleotides attached to gold nanocrystals probed by gel electrophoresis, Nano Lett. 3 (2003) 33–36, https://doi.org/10.1021/nl025888z.

[19] A. Sánchez Visedo, J. Losada-Matías, A.B. Soldado Cabezuelo, J.M. Costa Fernández, M.T. Fernández Fernández-Argüelles, M. Valledor Llopis, J.C. Campo Rodríguez, F.J. Ferrero Martín, A portable device for miRNAs detection based on a gold-nanoparticle ratiometric colorimetric strategy, IEEE Trans. Instrum. Meas. 71 (2022) 1–9, https://doi.org/10.1109/TIM.2022.3193426.

[20] A.R. Montoro Bustos, J. Ruiz Encinar, M.T. Fernández Fernández-Argüelles, J. M. Costa Fernández, A. Sanz-Medel, Elemental mass spectrometry: a powerful tool for an accurate characterisation at elemental level of quantum dots, Chem. Commun. 21 (2009) 3107–3109, https://doi.org/10.1039/b901493d.

[21] J.M. Costa Fernández, M. Menéndez-Miranda, D. Bouzas Ramos, J. Ruiz-Encinar, A. Sanz-Medel, Mass spectrometry for the characterization and quantification of engineered inorganic nanoparticles, Trac. Trends Anal. Chem. 84 (2016) 139–148, https://doi.org/10.1016/j.trac.2016.06.001.

[22] H. Hinterwirth, S. Kappel, T. Waitz, T. Prohaska, W. Lindner, M. Lämmerhofer, Quantifying thiol ligand density of self-assembled monolayers on gold nanoparticles by inductively coupled plasma–mass spectrometry, ACS Nano 7 (2013) 1129–1136, https://doi.org/10.1021/nn306024a.

[23] M. Matczuk, J. Legat, S.N. Shtykov, M. Jarosz, A.R. Timerbaev, Characterization of the protein corona of gold nanoparticles by an advanced treatment of CE-ICP-MS data, Electrophoresis 37 (2016) 2257–2259, https://doi.org/10.1002/elps.201600152.

[24] M. Menendez-Miranda, M.T. Fernandez-Arguelles, J.M. Costa-Fernandez, J. Ruiz-Encinar, A. Sanz-Medel, Elemental ratios for characterization of quantum-dots populations in complex mixtures by asymmetrical flow field-flow fractionation on-line coupled to fluorescence and inductively coupled plasma mass spectrometry, Anal. Chim. Acta 839 (2014) 8–13, https://doi.org/10.1016/j.aca.2014.06.034.

[25] D. Bouzas-Ramos, J.I. García-Alonso, J.M. Costa-Fernández, J. Ruiz-Encinar, Quantitative assessment of individual populations present in nanoparticle-antibody conjugate mixtures using AF4-ICP-MS/MS, Anal. Chem. 91 (2019) 3567–3574, https://doi.org/10.1021/acs.analchem.8b05482.